


Article

Synuclein Deficiency Results in Age-Related Respiratory and Cardiovascular Dysfunctions in Mice

Patrick S. Hosford¹, Natalia Ninkina^{2,3}, Vladimir L. Buchman^{2,3}, Jeffrey C. Smith⁴,
Nephtali Marina¹ and Shahriar SheikhBahaei^{4,5,*} 

¹ Department of Neuroscience Physiology and Pharmacology, Center for Cardiovascular and Metabolic Neuroscience, University College London (UCL), London WC1E 6BT, UK; p.hosford@ucl.ac.uk (P.S.H.); n.marina@ucl.ac.uk (N.M.)

² School of Biosciences, Cardiff University, Cardiff CF10 3AX, UK; ninkinan@cf.ac.uk (N.N.); buchmanvl@cf.ac.uk (V.L.B.)

³ Institute of Physiologically Active Compounds, Russian Academy of Sciences (IPAC RAS), 1 Severniy proezd, 142432 Chernogolovka, Moscow Region, Russia

⁴ Cellular and Systems Neurobiology Section, National Institute of Neurological Disorders and Stroke (NINDS), National Institutes of Health (NIH), Bethesda, MD 20892, USA; SmithJ2@ninds.nih.gov

⁵ Neuron-Glia Signaling and Circuits Unit, National Institute of Neurological Disorders and Stroke (NINDS), National Institutes of Health (NIH), Bethesda, MD 20892, USA

* Correspondence: sheikhbahaeis@ninds.nih.gov; Tel.: +1-301-496-4960; Fax: +1-301-496-1339

Received: 17 July 2020; Accepted: 20 August 2020; Published: 24 August 2020



Abstract: Synuclein (α , β , and γ) proteins are highly expressed in presynaptic terminals, and significant data exist supporting their role in regulating neurotransmitter release. Targeting the gene encoding α -synuclein is the basis of many animal models of Parkinson's disease (PD). However, the physiological role of this family of proteins is not well understood and could be especially relevant as interfering with accumulation of α -synuclein level has therapeutic potential in limiting PD progression. The long-term effects of their removal are unknown and given the complex pathophysiology of PD, could exacerbate other clinical features of the disease, for example dysautonomia. In the present study, we sought to characterize the autonomic phenotypes of mice lacking all synucleins (α , β , and γ ; $\alpha\beta\gamma^{-/-}$) in order to better understand the role of synuclein-family proteins in autonomic function. We probed respiratory and cardiovascular reflexes in conscious and anesthetized, young (4 months) and aged (18–20 months) $\alpha\beta\gamma^{-/-}$ male mice. Aged mice displayed impaired respiratory responses to both hypoxia and hypercapnia when breathing activities were recorded in conscious animals using whole-body plethysmography. These animals were also found to be hypertensive from conscious blood pressure recordings, to have reduced pressor baroreflex gain under anesthesia, and showed reduced termination of both pressor and depressor reflexes. The present data demonstrate the importance of synuclein in the normal function of respiratory and cardiovascular reflexes during aging.

Keywords: aged mouse; baroreflex; hypoxia; hypercapnia; Parkinson's disease; synuclein

1. Introduction

Synucleins (α , β , and γ) are a family of highly-conserved vertebrate-specific proteins, specifically enriched in pre-synaptic terminals of neurons and thought to be involved in regulating vesicular release and recycling of neurotransmitters [1–3]. The alpha-synuclein (α -syn) member of this family has come under intense research scrutiny because the pathophysiology of Parkinson's disease (PD) is particularly linked with α -syn abnormalities due to the discovery of a rare form of familial PD that was mapped to a single nucleotide change in the α -syn gene [4]. Subsequently, genome-wide association studies (GWAS) found α -syn to be the most relevant gene in cases of idiopathic PD. This led to the development of

numerous animal models of PD based on the mutation or over-expression of α -syn [5]. Additionally, there is an important role of α -syn in regulation of key stages of dopamine release, reuptake and recycling [6]. However, despite playing such an important role in pathology, surprisingly little was known about the physiological role of this protein. This was, in part, due to the sequence homology of the genes encoding the three members of this protein family [7,8]. The pattern of expression, predominantly in neuronal tissues, of these three proteins also has significant overlap, and while some tissues may express more than one member, generally all three are expressed simultaneously [9]. Synucleins seem to operate in redundancy as in single or double syn-knockout mice display decline in striatal dopamine and impaired synaptic function over time [10–12]. However, $\alpha\beta\gamma$ -syn triple-knockout ($\alpha\beta\gamma^{-/-}$) mice displayed a more severe age-dependent phenotype in comparison to single or double knockouts [2,7,13,14].

Autonomic deficits in PD are well-known to contribute to the overall pathology [15–17] but have recently received renewed attention because this dysfunction may precede the onset of motor symptoms [18–20]. Understanding how autonomic dysfunction associated with PD can be better treated or used for diagnosis requires studies with animal models. Indeed, both toxin-based animal models and those that rely on the (over)expression of (human) α -syn have been shown to recapitulate many of the features of PD dysautonomia [21]. Recently, reducing α -synuclein level has gained attention as a therapeutic method to limit the progression of PD [12]; however, experimental evidence on the long-term effects of removing α -synuclein on the development and normal function of the autonomic nervous system is lacking. Accordingly, in the present study, we sought to characterize the respiratory and cardiovascular phenotype of $\alpha\beta\gamma^{-/-}$ animals in order to better understand the role of this protein family in homeostatic autonomic cardiorespiratory responses.

2. Methods

2.1. Ethical Approval

All experiments were performed in accordance with the European Commission Directive 86/609/EEC (European Convention for the Protection of Vertebrate Animals used for Experimental and Other Scientific Purposes), the UK Home Office (Scientific Procedures) Act (1986), and the US National Institutes of Health Guide for the Care and Use of Laboratory Animals, with project approval from the respective Institutional Animal Care and Use Committees.

2.2. Generation of Single-, Double- and Triple-Synuclein-Null Mutant Animals

Generation of the $\alpha\beta\gamma$ -synuclein triple-knockout ($\alpha\beta\gamma^{-/-}$) mouse line has been described previously [14]. All animals were on the same C57Bl/6 genetic background. Briefly, lines of single synuclein knockout animals were backcrossed with C57Bl/6J mice for more than eight generations. Intercrossing the resultant animals produced double synuclein knockout and finally, $\alpha\beta\gamma^{-/-}$ mice. Wild-type (WT) littermates were used as controls. Young (3–4 months) and aged (18–20 months) male mice used in this study were housed in a temperature-controlled facility with a normal light–dark cycle (12 h:12 h, lights on at 7:00 am). Access to food (standard laboratory rodent diet) and water was provided ad libitum.

2.3. Physiological Experiments in Conscious Mice

2.3.1. Non-Invasive Breathing Measurement

Respiratory parameters were measured in unrestrained conscious mice by whole-body plethysmography as described previously [22,23]. Briefly, the mouse was placed in a Plexiglas recording chamber (~200 mL) that was flushed continuously with room air (unless otherwise required by the protocol) at a rate of 0.3 L min⁻¹. The animals were allowed to acclimatize to the chamber environment for ~30 min in room air. After baseline ventilation was measured, the O₂ concentration in

the chamber and thus inspired air was reduced to 15% and 10% for 5 min at each O₂ level. Similarly, in separate experiments, hyperoxic (~33% O₂) hypercapnia was induced by incrementally increasing the concentration of CO₂ in the chamber respiratory gas mixture to 3%, 6%, and 9%. Each CO₂ concentration was maintained for 5 min. Concentrations of CO₂ in the chamber were monitored online using a fast-response O₂/CO₂ analyzer (Morgan Medical, Hertford, UK). Respiratory rate (f_R , breaths per minute) and tidal volume (V_T , normalized per kilogram of body weight) were determined by the pressure changes in the chamber as described before [23,24]. The pressure signal was amplified, filtered, recorded, and analyzed offline using *Spike2* software (Cambridge Electronic Design, Cambridge, UK). The measurements of these ventilatory variables were obtained during the last 1–2 min of baseline recordings (i.e., before exposure to the gas mixtures) and during a 2 min period near the termination of each hypoxia or hypercapnia stimulus when the breathing pattern was stabilized. Hypoxia- or hypercapnia-induced changes in f_R , V_T , and minute ventilation ($V_E = f_R \times V_T$) were analyzed from the recordings.

2.3.2. Non-Invasive Blood Pressure Measurement

Non-invasive blood pressure measurements were conducted in conscious mice of all strains by means of an integrated tail-cuff plethysmography system (CODA system, Kent Scientific, Torrington, CT, USA; [25]). Blood pressure measurements were performed by the same investigator and at the same time of day for all mice within each experimental group. Mice were moved to a quiet, temperature-controlled area 12 h before measurements commenced. Air temperature was between 32 and 34 °C, thermoneutral for rodents, in order to ameliorate increases in sympathetic drive associated with cold stress [26]. Animals were restrained in a tube with nose-cone attachment (Kent Scientific) and placed on a heated platform at 37 °C. The tail was instrumented with a cuff and volume-pressure recording sensor. At least ten consecutive volume–pressure measurements were taken over a period of 15 min and averaged to determine resting arterial blood pressure and heart rate. Measurements were repeated the following day and all variables reported are an average of two consecutive measurement periods.

2.4. Anesthetized Preparation for Baroreflex Measurements

2.4.1. Surgical Preparation

Mice were anesthetized with urethane (ethyl carbamate; 1.2 g kg⁻¹, i.p.) and both the left common carotid artery and right jugular vein were cannulated using fine-bore polyethylene tubing (ID.38 OD 1.09 mm; Smith's Medical, Kent, UK) filled with heparinized saline. Mice were allowed to freely breathe room air and placed on a homeothermic heating pad to maintain body temperature at 37 ± 5 °C. The arterial cannula was connected to a pressure transducer for measurement of blood pressure. Depth of anesthesia was assessed by absence of withdrawal from paw-pinch and the stability of blood pressure and heart rate recorded. Additionally, two subcutaneous electrodes were placed on left and right flanks for recording of ECG. Signals were amplified and filtered (High-pass 50 Hz, low-pass 20 kHz) using a Neurolog System (Digitimer, Welwyn Garden City, UK). Recordings of the physiological variables obtained in anesthetized animals were digitized using a Cambridge Electronic Design (CED) power1401 interface and analyzed using *Spike2* software.

2.4.2. Baroreflex Protocol

After allowing the animal to stabilize approximately 10 min following surgery, the baroreflex protocol was started. Animals were subjected to three randomized doses of phenylephrine (5, 10 and 25 µg per animal) and/or sodium nitroprusside (5, 15 and 30 µg per animal). Drugs were administered slowly over 5–10 s via the jugular vein cannula in volumes that did not exceed 50 µL. Maximum changes in mean arterial blood pressure and R-R interval were calculated from the blood pressure and ECG trace, respectively. Baroreflex gain was calculated by the change in heart rate divided by the

change in blood pressure. Additionally, the ‘overshoot’ in heart rate and systolic blood pressure after returning to baseline following activation of the pressor reflex and depressor reflexes was assessed.

2.4.3. Morphometries

At the end of the experiment, animals were humanely sacrificed with an overdose of pentobarbital sodium (30 mg kg⁻¹). The heart was rapidly removed and rinsed with saline. Total heart weight was measured and then the left ventricle was carefully dissected free of the remaining tissue under microscopic guidance and weighed.

2.5. Data Analysis

Data are reported as mean \pm SEM and plotted as individual points using Prism 8 (GraphPad Inc., San Diego, CA, USA). Datasets were tested for normality using a Shapiro–Wilk normality test and were compared by Kruskal–Wallis ANOVA by ranks, Mann–Whitney *U* rank test, or Wilcoxon matched-pairs signed-rank test as appropriate. Differences between groups with $p < 0.05$ were considered significant.

3. Results

3.1. Respiratory Activity in Conscious Mice

3.1.1. Resting Breathing in Room Air and Hyperoxic Condition

The resting breathing frequency (f_R) of young $\alpha\beta\gamma^{-/-}$ mice in room air (i.e., normoxia/normocapnia) was higher when compared to the wild-type mice ($241 \pm 17 \text{ min}^{-1}$ ($n = 8$) vs. $166 \pm 11 \text{ min}^{-1}$ ($n = 7$); $p = 0.014$, Mann–Whitney *U* rank test; Figure 1A). Similarly, with $\alpha\beta\gamma^{-/-}$ aged mice, f_R remained higher ($259 \pm 15 \text{ min}^{-1}$ ($n = 10$) vs. $195 \pm 13 \text{ min}^{-1}$ ($n = 9$) than age-matched wild-type mice; $p = 0.010$; Figure 1B). However, in the hyperoxia/normocapnia condition ($\sim 33\%$ O₂ in the inspired air), f_R was not different in younger mice ($245 \pm 6 \text{ min}^{-1}$ ($n = 8$) vs. $251 \pm 8 \text{ min}^{-1}$ ($n = 7$); $p = 0.44$, Mann–Whitney *U* rank test; Figure 1A), but in this condition, f_R remained higher (by 24%) in aged $\alpha\beta\gamma^{-/-}$ mice ($268 \pm 13 \text{ min}^{-1}$ ($n = 10$) vs. $204 \pm 15 \text{ min}^{-1}$ ($n = 9$); $p = 0.001$, Mann–Whitney *U* rank test; Figure 1B).

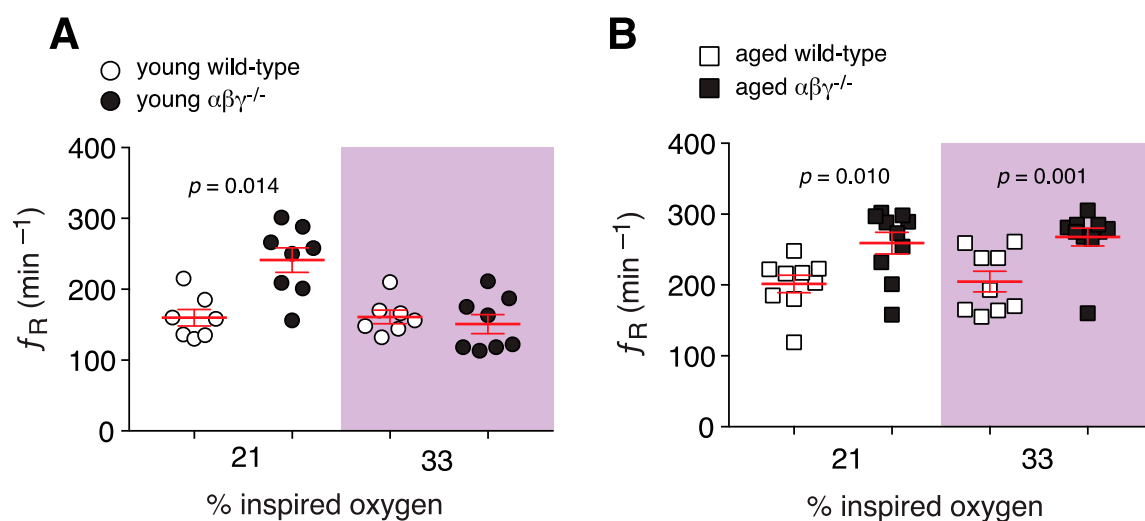


Figure 1. $\alpha\beta\gamma^{-/-}$ mice display age-dependent increases in resting breathing frequency in normoxia and hyperoxia. (A,B) Population data from whole-body plethysmography measurements showing respiratory rate (f_R) in young (A) and aged (B) WT and $\alpha\beta\gamma^{-/-}$ mice at room air (21% O₂) and hyperoxic conditions (33% O₂). p —Mann–Whitney *U* rank test.

3.1.2. Ventilatory Response to Hypoxia

f_R , V_T , and V_E responses during mild hypoxic challenges (15% O₂ in the inspired air) were not different in young or aged transgenic mice when compared to their wild-type counterparts (data not shown). However, when challenged with moderate hypoxia (10% O₂ in the inspired air), f_R increased in young wild-type mice by ~41% ($234 \pm 10 \text{ min}^{-1}$ vs. $166 \pm 11 \text{ min}^{-1}$ in room air, $n = 7$; $p = 0.016$, Wilcoxon matched-pairs signed-rank test; Figure 2A). In contrast, during hypoxia, f_R decreased in young $\alpha\beta\gamma^{-/-}$ animals (by ~8%, $222 \pm 17 \text{ min}^{-1}$ vs. $241 \pm 16 \text{ min}^{-1}$ in room air, $n = 8$; $p = 0.047$, Wilcoxon matched-pairs signed-rank test; Figure 2A). Despite this decrease in f_R , the hypoxia-induced f_R in young $\alpha\beta\gamma^{-/-}$ animals was not different from wild-type ($p = 0.7$, Mann–Whitney U rank test; Figure 2B). Hypoxic challenge increased tidal volume (V_T) by ~37% in wild-type ($2.5 \pm 0.2 \text{ a.u.}$ vs. $1.8 \pm 0.1 \text{ a.u.}$ in normoxia; $p = 0.016$, Wilcoxon matched-pairs signed-rank test) and by ~20% in $\alpha\beta\gamma^{-/-}$ animals ($2.4 \pm 0.2 \text{ a.u.}$ vs. $1.8 \pm 0.1 \text{ a.u.}$ at normoxia, $p = 0.039$, Wilcoxon matched-pairs signed-rank test; Figure 2B). However, the magnitude of the hypoxic V_T was not different between groups. In addition, hypoxia-induced minute ventilation (V_E) was quantitatively similar between young wild-type and $\alpha\beta\gamma^{-/-}$ mice ($525 \pm 42 \text{ a.u.}$ vs. $578 \pm 73 \text{ a.u.}$ in wild-type; $p = 0.5$, Mann–Whitney U rank test; Figure 2B).

In aged $\alpha\beta\gamma^{-/-}$ animals, hypoxia did not affect f_R ($259 \pm 15 \text{ min}^{-1}$ vs. $260 \pm 12 \text{ min}^{-1}$ in room air, $n = 10$; $p = 0.77$, Wilcoxon matched-pairs signed-rank; Figure 2C). Although hypoxia increased f_R in aged wild-type mice by ~37% ($271 \pm 12 \text{ min}^{-1}$ vs. $195 \pm 13 \text{ min}^{-1}$ in room air, $n = 9$; $p = 0.004$, Wilcoxon matched-pairs signed-rank; Figure 2C), the hypoxic breathing rate was not different between aged $\alpha\beta\gamma^{-/-}$ and wild-type mice ($260 \pm 12 \text{ min}^{-1}$ vs. $271 \pm 12 \text{ min}^{-1}$ in wild-type; $p = 0.55$, Mann–Whitney U rank test; Figure 2D). During hypoxia V_T was also increased in aged wild-type mice by ~19% ($2.2 \pm 0.1 \text{ a.u.}$ vs. $1.9 \pm 0.1 \text{ a.u.}$ at normoxia, $n = 10$; $p = 0.037$, Wilcoxon matched-pairs signed-rank test). However, hypoxia did not cause a significant increase in V_T in aged $\alpha\beta\gamma^{-/-}$ animals ($1.97 \pm 0.1 \text{ a.u.}$ vs. $1.91 \pm 0.1 \text{ a.u.}$ at normoxia, $n = 12$; $p = 0.52$, Wilcoxon matched-pairs signed-rank test; Figure 2B). As opposed to younger mice, hypoxia-induced V_E was decreased in aged $\alpha\beta\gamma^{-/-}$ animals ($513 \pm 44 \text{ a.u.}$ vs. $651 \pm 31 \text{ a.u.}$ in wild-type; $p = 0.016$, Mann–Whitney U rank test; Figure 2B).

3.1.3. Ventilatory Response to Hypercapnia

f_R , V_T , and V_E responses during mild hypercapnic challenges (3% CO₂ in the inspired air) were not different in young or aged transgenic mice when compared to their wild-type counterparts (data not shown). Similarly, there were no differences in respiratory responses to moderate hypercapnia challenge (6% CO₂ in the inspired air) and severe hypercapnia challenge (9% CO₂ in the inspired air) between young $\alpha\beta\gamma^{-/-}$ and wild-type mice (Figure 3A,B). However, compared to aged-wild-type mice, aged $\alpha\beta\gamma^{-/-}$ mice displayed impaired CO₂-induced augmentation of f_R in 6% CO₂ ($291 \pm 7 \text{ min}^{-1}$ vs. $268 \pm 13 \text{ min}^{-1}$ in normocapnia, $n = 10$; $p = 0.08$, Wilcoxon matched-pairs signed-rank test) and 9% CO₂ ($313 \pm 11 \text{ min}^{-1}$ vs. $268 \pm 13 \text{ min}^{-1}$ in normocapnia, $n = 10$; $p = 0.004$, Wilcoxon matched-pairs signed-rank test; Figure 3C). In addition, CO₂-induced f_R in aged $\alpha\beta\gamma^{-/-}$ mice was found to be lower by 12% [$291 \pm 7 \text{ min}^{-1}$ ($n = 10$) vs. $332 \pm 13 \text{ min}^{-1}$ in wild-type ($n = 9$); $p = 0.023$, Mann–Whitney U rank test] and 20% [$313 \pm 11 \text{ min}^{-1}$ ($n = 10$) vs. $398 \pm 8 \text{ min}^{-1}$ in wild-type ($n = 9$); $p < 0.001$, Mann–Whitney U rank test], respectively (Figure 3D).

In addition, the CO₂-induced increase in V_E was lower in aged $\alpha\beta\gamma^{-/-}$ mice when challenged with 6 and 9% CO₂ by 23% ($834 \pm 62 \text{ a.u.}$ vs. $1077 \pm 97 \text{ a.u.}$ in wild-type; $p = 0.07$, Mann–Whitney U rank test) and 28% ($1414 \pm 63 \text{ a.u.}$ vs. $1974 \pm 105 \text{ a.u.}$ in wild-type; $p = 0.001$, Mann–Whitney U rank test; Figure 3D), respectively.

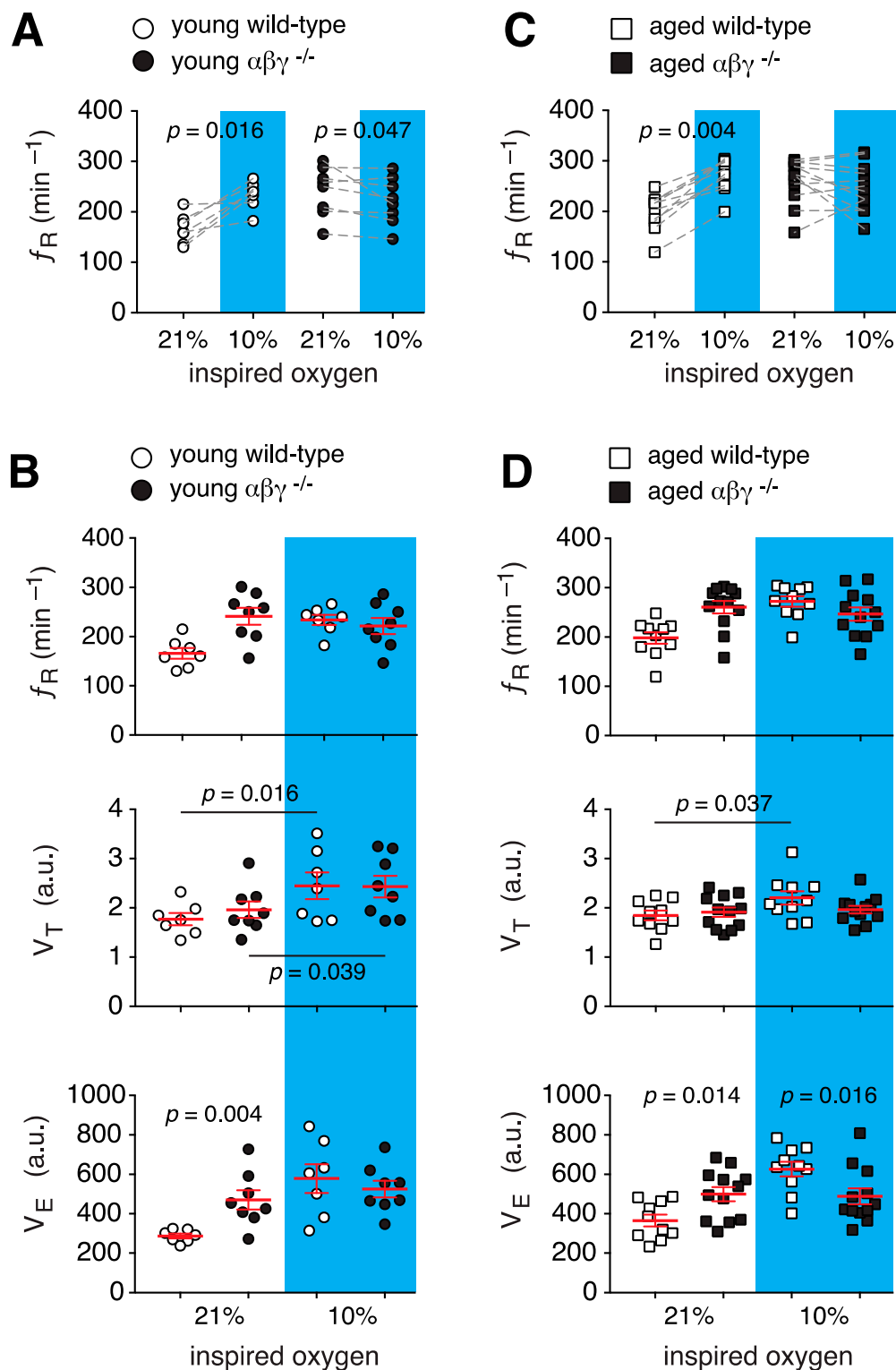


Figure 2. Respiratory responses of $\alpha\beta\gamma^{-/-}$ mice to hypoxia. (**A,B**) Group data from whole-body plethysmography measurements of respiratory rate (f_R), tidal volume (V_T), and minute ventilation (V_E) of unrestrained young wild-type and $\alpha\beta\gamma^{-/-}$ mice in room air (21% O_2) and moderate hypoxia (10% O_2). (**C,D**) Summary data from whole-body plethysmography measurements of breathing parameters (f_R , V_T , V_E) of aged wild-type and $\alpha\beta\gamma^{-/-}$ mice in 21% and 10% O_2 . p —Wilcoxon matched-pairs signed-rank test (**A,C**), middle panels in (**B,D**); Mann–Whitney U rank test (lower panels in (**B,D**)).

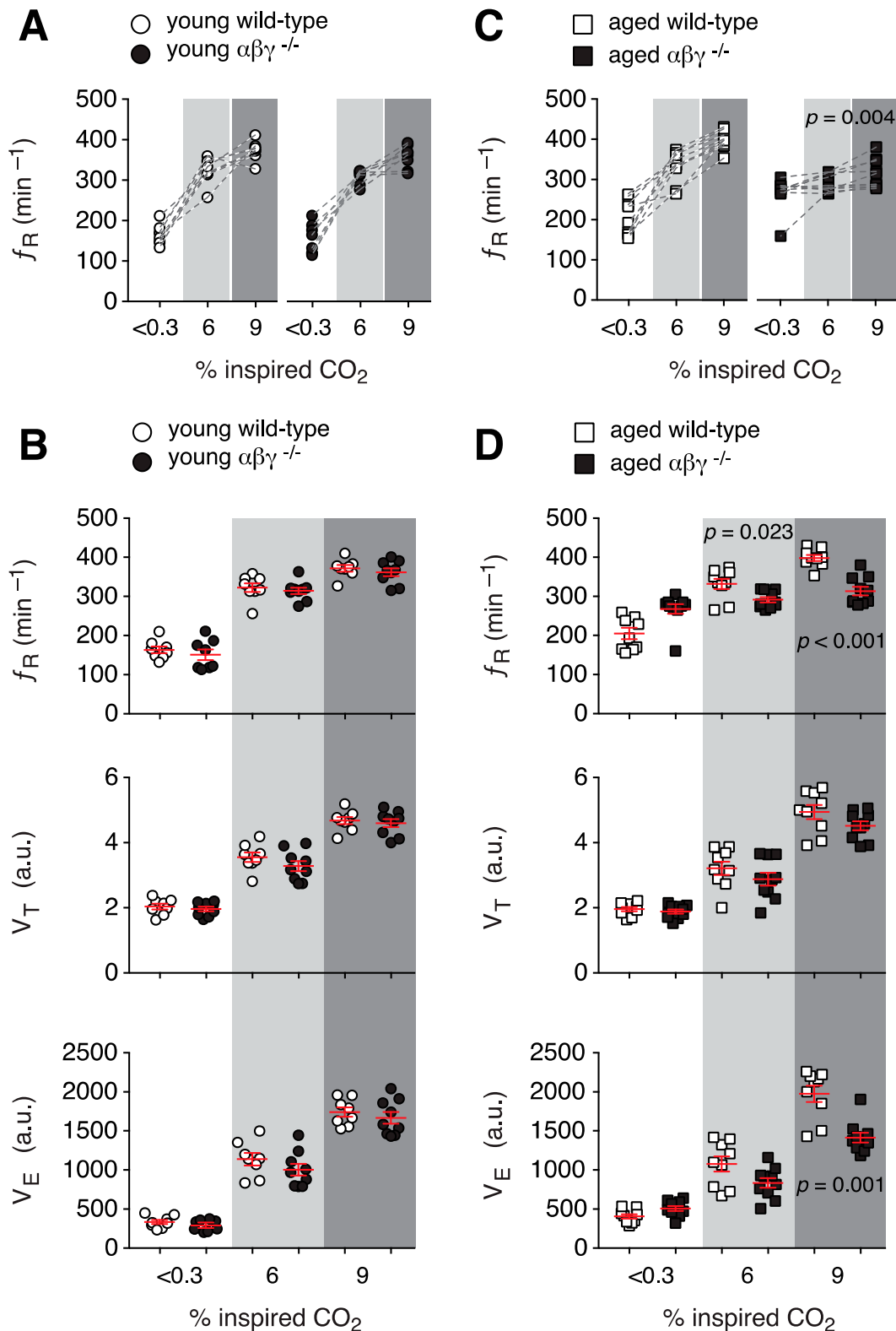


Figure 3. Respiratory responses of $\alpha\beta\gamma^{-/-}$ mice to hypercapnia. (A,B) Group data from whole-body plethysmography measurements of respiratory rate (f_R), tidal volume (V_T), and minute ventilation (V_E) of unrestrained young wild-type and $\alpha\beta\gamma^{-/-}$ mice in $< 0.03\%$ CO_2 , mild (6% CO_2), and moderate hypercapnia (9% CO_2). (C,D) Summary data from whole-body plethysmography measurements of breathing parameters (f_R , V_T , V_E) of aged wild-type and $\alpha\beta\gamma^{-/-}$ mice in $< 0.03\%$, 6% , and 9% CO_2 . p —Wilcoxon matched-pairs signed-rank test (C); Mann-Whitney U rank test (D).

3.2. Heart Morphometry Parameters

Heart morphometry measurements were taken from both aged and young $\alpha\beta\gamma^{-/-}$ mice. Body, heart and left ventricle weights were recorded and heart to body weight ratio was calculated. No significant differences ($p > 0.05$, Mann–Whitney U rank test) between phenotypes in either age groups were detected (Table 1).

Table 1. Comparison of morphometric parameters between $\alpha\beta\gamma^{-/-}$ and wild-type control animals for both young and aged groups. Means \pm S.E.M were compared with Mann–Whitney U rank test.

	Young Wild Type	Young $\alpha\beta\gamma^{-/-}$	p Value	Aged Wild Type	Aged $\alpha\beta\gamma^{-/-}$	p Value
n	6	6		6	6	
Body Weight (g)	26.8 \pm 0.5	28.2 \pm 0.6	0.13	27.2 \pm 0.7	25.6 \pm 0.8	0.08
Heart Weight (g)	0.156 \pm 0.005	0.157 \pm 0.006	0.85	0.183 \pm 0.2	0.157 \pm 0.01	0.18
LV Weight (g)	0.088 \pm 0.006	0.091 \pm 0.002	0.79	0.113 \pm 0.1	0.092 \pm 0.005	0.14
HW/BW Ratio	5.78 \pm 0.04	5.59 \pm 0.20	0.23	6.71 \pm 0.5	6.39 \pm 0.4	0.53

3.3. Hemodynamics in Conscious Mice

In young animals, no differences in blood pressure or heart rate were detected between genotypes in any variable measured ($p > 0.05$, Mann–Whitney U rank test; Table 2). However, resting systolic, diastolic and MAP were all significantly ($p = 0.015$, Mann–Whitney U rank test) higher in aged $\alpha\beta\gamma^{-/-}$ compared to wild-type animals (Table 2), though basal heart rate was not different between genotypes in aged mice. Furthermore, we found no significant difference in hemodynamic measurements between single synuclein-null ($\alpha^{-/-}$, $\beta^{-/-}$, $\gamma^{-/-}$) and the double synuclein-null ($\alpha\gamma^{-/-}$) animals when compared to the aged control group (Table 3).

Table 2. Hemodynamic parameters measured using tail-cuff plethysmograph in conscious $\alpha\beta\gamma^{-/-}$ and wild-type control animals for both young and aged groups. Means \pm S.E.M were compared with Mann–Whitney U rank test.

	Young Wild Type	Young $\alpha\beta\gamma^{-/-}$	p Value	Aged Wild Type	Aged $\alpha\beta\gamma^{-/-}$	p Value
n	8	9		8	8	
Diastolic BP (mmHg)	86.7 \pm 4.2	87.8 \pm 3.4	0.94	121 \pm 5.9	147 \pm 6.9	0.02
Systolic BP (mmHg)	121.9 \pm 5.1	125.0 \pm 3.6	0.72	161 \pm 7.0	185 \pm 7.0	0.02
Mean BP (mmHg)	98.1 \pm 4.4	99.8 \pm 3.4	0.87	133.9 \pm 6.2	159.5 \pm 6.9	0.02
Heart rate (bpm)	568 \pm 33	572.0 \pm 19	0.73	599 \pm 37	632 \pm 9	0.92

Table 3. Hemodynamic parameters measured using tail-cuff plethysmograph in conscious aged single synuclein-null ($\alpha^{-/-}$, $\beta^{-/-}$, $\gamma^{-/-}$) and the double synuclein-null ($\alpha\gamma^{-/-}$) animals. Means \pm S.E.M were compared with Mann–Whitney *U* rank test.

	Aged Wild Type	Aged $\alpha^{-/-}$	<i>p</i> Value	Aged $\beta^{-/-}$	<i>p</i> Value	Aged $\gamma^{-/-}$	<i>p</i> Value	Aged $\alpha\gamma^{-/-}$	<i>p</i> Value
<i>n</i>	8	3		5		3		3	
Diastolic BP (mmHg)	119 \pm 7	130 \pm 6	0.38	137 \pm 6	0.093	118 \pm 8	0.667	120 \pm 5	0.67
Systolic BP (mmHg)	159 \pm 6	163 \pm 5	0.92	171 \pm 6	0.617	152 \pm 7	0.170	155 \pm 6	0.17
Mean BP (mmHg)	132 \pm 6	141 \pm 5	0.63	148 \pm 6	0.127	129 \pm 8	0.667	131 \pm 5	0.55
Heart rate (bpm)	572 \pm 45	636 \pm 38	>0.99	651 \pm 11	0.343	625 \pm 49	0.667	601 \pm 19	0.33

Interestingly, we found both aged wild-type and the TKO mice were significantly hypertensive compared to their young counterparts. Resting systolic, diastolic and MAP, but not heart rate, were all significantly ($p < 0.001$, Mann–Whitney *U* rank test) higher in the aged vs. the young wild-type mice.

3.4. Hemodynamics under Anesthesia

Systolic, diastolic, mean arterial pressure and heart rate were measured over a 5-min period immediately prior to commencement of the baroreflex protocol. Under anesthesia, there was no significant difference detected in any parameter between genotypes ($p < 0.05$; Mann–Whitney *U* rank test; Table 4).

Table 4. Hemodynamic parameters measured under urethane anesthesia (1.2 g kg⁻¹, i.v.) in $\alpha\beta\gamma^{-/-}$ and wild-type control animals for both young and aged groups. Means \pm S.E.M were compared with Mann–Whitney *U* rank test.

	Young Wild Type	Young $\alpha\beta\gamma^{-/-}$	<i>p</i> Value	Aged Wild Type	Aged $\alpha\beta\gamma^{-/-}$	<i>p</i> Value
<i>n</i>	5	5		8	8	
Diastolic BP (mmHg)	78 \pm 4	80 \pm 5	0.67	72 \pm 3	79 \pm 4	0.71
Systolic BP (mmHg)	107 \pm 3	109 \pm 5	0.74	96 \pm 4.0	94 \pm 5	0.77
Mean BP (mmHg)	65 \pm 5	67 \pm 5	0.65	83 \pm 4	85 \pm 4	0.92
Heart rate (bpm)	658 \pm 7	623 \pm 22	0.22	575 \pm 33	626 \pm 25	0.36

3.5. Baroreflex

3.5.1. Baroreflex Sensitivity

Baroreflex sensitivity was assessed over a range of blood pressure changes from -30 to $+50$ mmHg (Figure 4). No significant differences in either the pressor or the depressor reflex were detected in the young animals between genotypes (Figure 4A,B). In aged animals, the pressor reflex was found to be significantly attenuated in $\alpha\beta\gamma^{-/-}$ subjects (1.1 ± 0.2 ($n = 12$) vs. 0.6 ± 0.1 bpm mmHg⁻¹ ($n = 8$) compared to aged wild-type mice; Figure 4C, $p = 0.02$, Mann–Whitney *U* rank test). However, there was no difference found ($p = 0.84$; Mann–Whitney *U* rank test) in depressor reflex gain between aged $\alpha\beta\gamma^{-/-}$ and aged wild-type animals (-5.3 ± 0.3 ($n = 6$) vs. -5.3 ± 0.3 bpm mmHg⁻¹ ($n = 6$, Figure 4D)).

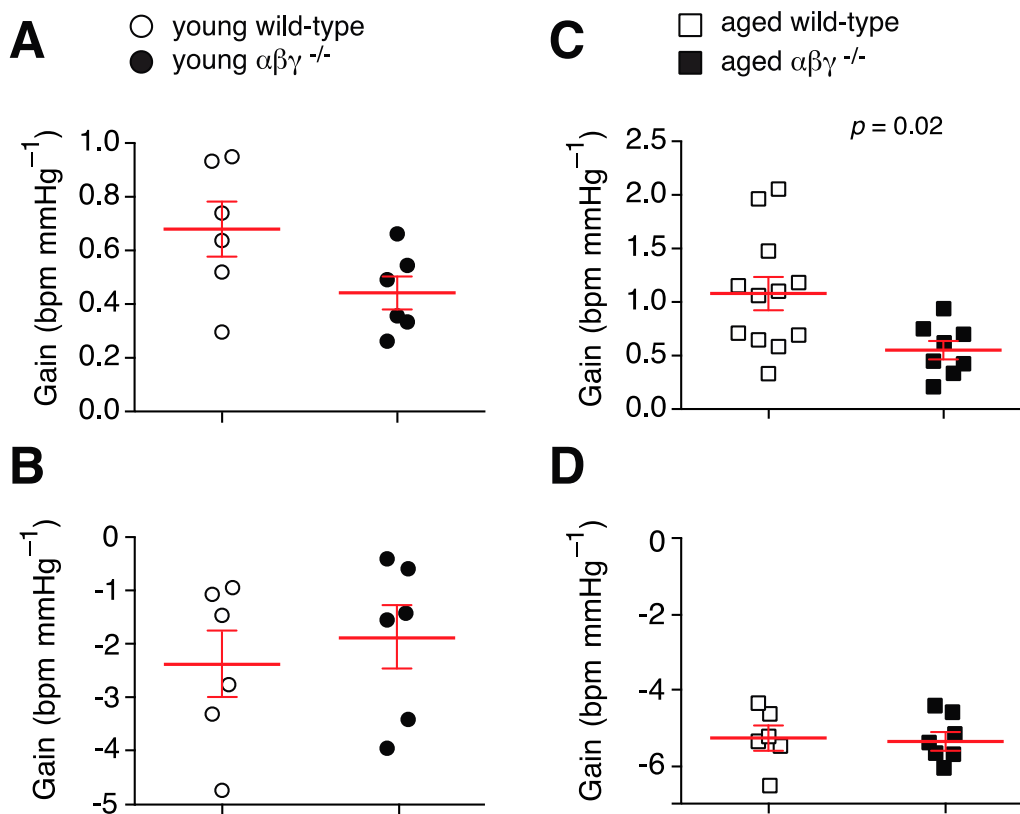


Figure 4. Comparisons of baroreflex gain in wild-type and $\alpha\beta\gamma^{-/-}$ mice. (A) Depressor reflex in aged mice. (B) Pressor reflex in aged mice. (C) Depressor reflex in young mice. (D) Pressor reflex in young mice. Means \pm S.E.M were compared with Mann–Whitney U rank test.

3.5.2. Baroreflex Recovery

In order to gain a more complete understanding of how $\alpha\beta\gamma$ -synuclein deletion affects baroreflex, the recovery period after baroreflex activation was also analyzed. Following activation of the depressor reflex, restoration of heart rate was assessed in terms of a maximum change from baseline. Similarly, following activation of pressor reflex, restoration of diastolic blood pressure was assessed in terms of a maximum change from baseline. Decreases in heart rate and decreases in blood pressure following activation of the depressor and pressor reflex, respectively, were matched across genotypes and the maximum change above baseline was calculated (Figure 5A,B). The $\alpha\beta\gamma^{-/-}$ mice displayed a significantly higher overshoot from baseline during heart rate restoration (57 ± 7 ($n = 5$) vs. 10 ± 3 bpm ($n = 5$) in wild-type mice; Figure 5C, $p = 0.008$, Mann–Whitney U rank test). TKO animals also displayed a significantly higher overshoot from baseline during systolic blood pressure recovery [6 ± 1 ($n = 4$) vs. 12 ± 1 mmHg ($n = 4$) in wild-type; Figure 5D, $p = 0.02$, Mann–Whitney U rank test]. Again, no differences were detected between genotypes in the young animals.

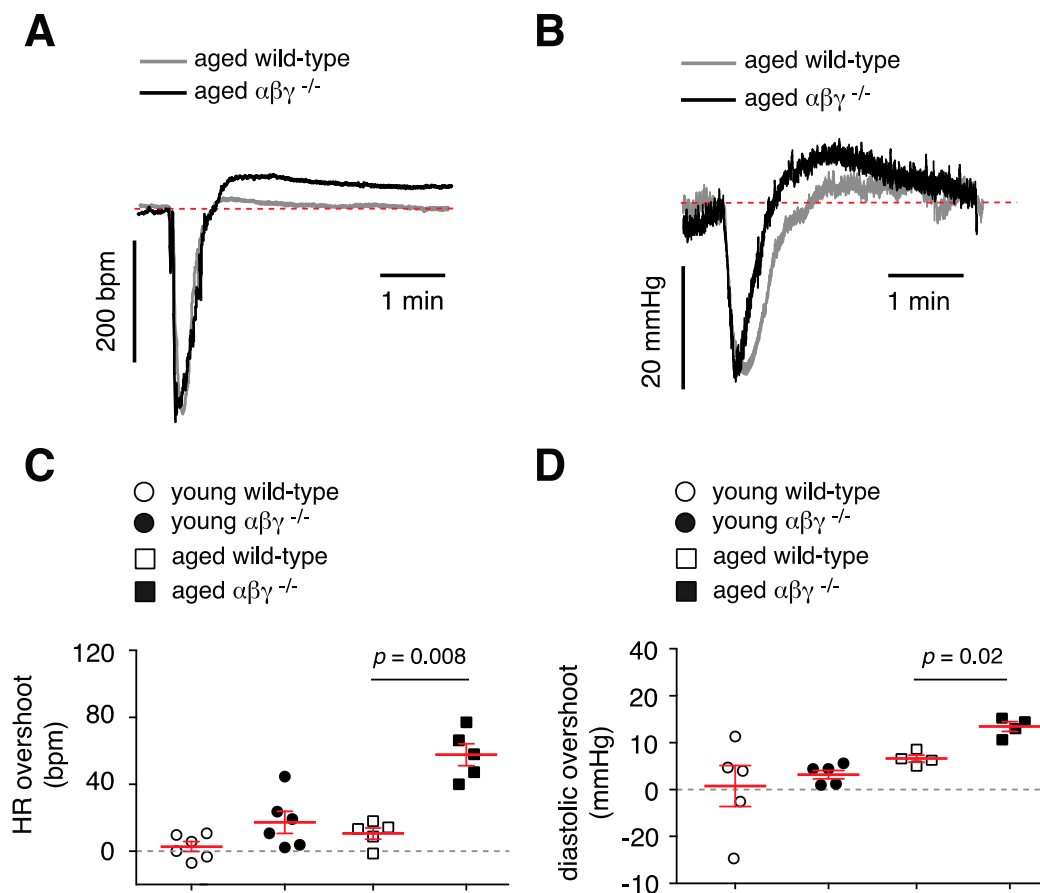


Figure 5. Heart rate and diastolic blood pressure restoration in $\alpha\beta\gamma^{-/-}$ mice. (A) Example trace showing heart rate after activation of the depressor reflex in aged wild-type and $\alpha\beta\gamma^{-/-}$ mice. (B) Example trace showing diastolic blood pressure after activation of the pressor reflex in aged wild-type and $\alpha\beta\gamma^{-/-}$ mice. (C) Combined data showing maximum change (overshoot) in heart rate above baseline after activation of the depressor reflex in aged, young wild-type and $\alpha\beta\gamma^{-/-}$ mice. (D) Combined data showing maximum change in diastolic blood pressure above baseline after activation of the pressor reflex in aged, young wild-type and $\alpha\beta\gamma^{-/-}$ mice. Means \pm S.E.M were compared with a Mann–Whitney U rank test.

4. Discussion

In the mammalian nervous system, the presence of other members of the synuclein proteins (i.e., β - and γ -synuclein) often makes physiological studies of functional roles of α -synuclein difficult. Therefore, synuclein triple-knockout ($\alpha\beta\gamma^{-/-}$) mice, by removing potential compensatory effects of β -syn and γ -syn, offers a good model to investigate the physiological function of α -syn in a synuclein-null, and an age-dependent setting [13]. Data from our study demonstrate that aged mice lacking $\alpha\beta\gamma$ -synuclein proteins have impaired respiratory responses to hypoxia and hypercapnia, elevated blood pressure, pressor reflex failure, and reduced ability to terminate both pressor and depressor reflex leading to overcompensation. Young $\alpha\beta\gamma^{-/-}$ mice showed compromised respiratory responses to hypoxic but not hypercapnic challenges. Mutations in α -syn are linked to Parkinson's disease [4,27–29], and $\alpha\beta\gamma^{-/-}$ mice have been used as a model to study age-dependent phenotypes in Parkinson's disease [4,13,30–33]. Moreover, recent data have linked impaired synuclein proteins to the mitochondrial dysfunction in Parkinson's disease [34–37].

4.1. Respiratory Function

Recently, we have shown that during hypoxic challenge, mitochondrial $\Delta\Psi_m$ in brainstem astrocytes decreases in which this depolarization of the $\Delta\Psi_m$ leads to release of ROS and eventually, increases in f_R [38]. Interestingly, in $\alpha\beta\gamma^{-/-}$ mice, hypoxia failed to increase f_R from baseline levels in both young and aged mice (Figure 2), which suggests that the brainstem of these mice is hypoxic and/or the central mechanism for low- O_2 sensing in these mice are impaired/activated [39]. Previously, we have shown that astrocytes in the ventrolateral medulla (VLM) by modulating activities of the respiratory rhythm-generating circuits of the preBötzinger complex [40,41] regulate the ventilatory response to hypoxia in an ATP-dependent manner [24,38,42]. We also showed that astroglial mitochondria can act as a central oxygen sensor [24,38]. Abnormal mitochondrial function was reported in $\alpha\beta\gamma^{-/-}$ mice, in which the mitochondrial membrane potential ($\Delta\Psi_m$) was found to be decreased (i.e., depolarized) in both astrocytes and neurons [43,44]. The fact that hyperoxia (33% O_2 in the inspired air) decreased f_R in younger $\alpha\beta\gamma^{-/-}$ mice but not the aged counterparts further strengthens this hypothesis.

As opposed to impaired age-independent respiratory responses to hypoxia, $\alpha\beta\gamma^{-/-}$ mice showed an age-dependent respiratory response to hypercapnia (6% and 9% CO_2 in the inspired air). Our results are in agreement with age-dependent data reported from 6-hydroxydopamine (6-OHDA)-model of Parkinson's disease [45–48] in which injection of 6-OHDA into the striatum/substantia nigra induced Parkinson's disease in rats [45] and mice [49], and these rats also exhibited an age-dependent impaired response to hypercapnic challenges. However, 6-OHDA rats showed normal augmentation of breathing when challenged with hypoxia [45]. The fact that respiratory responses to hypoxic challenge were normal in 6-OHDA rats but were impaired in $\alpha\beta\gamma^{-/-}$ mice (this study) can be explained by the fact that in the 6-OHDA model, the defect is only induced in neurons [45], but both neurons and astrocytes showed impaired mitochondrial function in the $\alpha\beta\gamma^{-/-}$ mice [43].

4.2. Cardiovascular Function

Conscious measurements of blood pressure show a clear age-dependent increase in mean arterial pressure in animals lacking all three synuclein sub-types (Table 2). The baroreflex (pressor reflex) was also found to be inhibited in aged animals, as well as an increased overshoot of both heart rate and blood pressure during the recovery phase of the pressor and depressor reflexes, respectively. We did not detect any differences in heart morphometry (Table 1) between the mouse strains that could compound any differences seen in cardiovascular physiology. This was in agreement with the other report of this strain of mice being phenotypically normal compared with wild types in size, weight and gross brain anatomy, up to 14 months of age [14]. Therefore, we suggest that the data indicates the features of the cardiovascular phenotype are neurogenic in origin.

Together, the cardiovascular phenotype suggests deletion of $\alpha\beta\gamma$ -synuclein produces a chronic reduction of parasympathetic (vagal) tone and inability to appropriately regulate sympathetic tone as previously indicated by altered cardiac parasympathetic control [50]. The impaired parasympathetic tone can explain the exacerbation of the age-related hypertension as seen in the aged wild-type animals (compared to the young wild-type) in the present study and reported previously [51]. Parasympathetic tone has been shown to be an important determinant of blood pressure in a model of hypertension, where chronic augmentation of parasympathetic tone has been shown to be anti-hypertensive [52]. Aging of the autonomic nervous system can be characterized as a generalized shifting of the sympathetic-parasympathetic balance [53] leading to various cardiovascular pathologies, including hypertension [54]. Deletion of $\alpha\beta\gamma$ -synuclein produces impairment of circuits controlling the autonomic nervous system that parallels the age-related synaptic dysfunction in the striatum [13,14] and as a result, exacerbates the shift from parasympathetic to the preponderance of sympathetic tone. This is supported by the autonomic symptoms occurring before or in parallel with the movement and cognitive symptoms of the synucleinopathies [55].

This pattern of autonomic dysfunction is also supported by the impaired baroreflex displayed by aged $\alpha\beta\gamma^{-/-}$ mice. Baroreflex activation maintains blood pressure and heart rate within narrow

physiological ranges through activation or withdrawal of central sympathetic and parasympathetic outflow in response to input from baroreceptors; decreases in blood pressure result in sympathetic activation and parasympathetic withdrawal, and blood pressure increases result in the opposite response.

The impaired pressor reflex suggests a similar dysfunction in sympathetic circuits or peripheral sympathetic signaling as sympathetic outflow must be engaged in order to restore blood pressure after it is lowered, as previously suggested [56]. Similarly, the failure of blood pressure and heart rate restoration following activation of either the pressor or depressor reflex further indicates a lack of appropriate autonomic control. This could be due to the lack of parasympathetic tone allowing sympathetic activation to dominate during baroreflex activation. This would cause an overshoot of heart rate by hyperactivation of cardiac beta-adrenoceptors when recovering from depressor reflex activation and similar inappropriate activation of vascular alpha-adrenoceptors. A similar pattern of baroreflex dysregulation was reported in mice that express a mutant form of α -synuclein [53], again suggesting that autonomic circuits are susceptible to the same pathology as seen in the striatum.

Interestingly, there was no differences in blood pressure detected in animals lacking a single synuclein or in the double ($\alpha\gamma$) knockout animals (Table 3). This suggests that there is a significant compensation between the three members of synuclein family as all three must be absent for increased blood pressure to be observed. This is in concordance with data of synaptic dysfunction in the striatum [14].

5. Summary and Conclusions

The present data support a role of synuclein in the normal function of the autonomic nervous system and central respiratory control during aging. Previous data have been collected using toxin-based models of overexpression of mutant α -synuclein proteins and have shown autonomic and respiratory deficits. However, until now, nothing has been known about the role of α -synuclein in normal autonomic physiology. We have shown $\alpha\beta\gamma^{-/-}$ mice have marked age-related respiratory and cardiovascular deficits. Our data suggest synuclein proteins are necessary for healthy aging in central respiratory and autonomic neuronal circuits and any treatment that reduces the availability of synuclein proteins over time may decrease the cardio-respiratory reflexes and worsen the treatment outcomes.

Author Contributions: P.S.H. and S.S. designed research; P.S.H. and S.S. performed research; V.L.B., N.N., J.C.S., N.M. contributed new reagents/analytic tools; P.S.H. and S.S. analyzed data; P.S.H. and S.S. wrote the paper. All authors have read and agreed to the published version of the manuscript.

Funding: This work was supported by The British Heart Foundation (N.M., FS/13/5/29927), Russian Science Foundation (V.L.B., 19-14-00064), and in part by the Intramural Research Program of the NIH, NINDS (J.C.S. and S.S.).

Acknowledgments: We thank Alexander Gourine for providing support for this study.

Conflicts of Interest: The authors declare no competing financial interest.

References

1. Clayton, D.F.; George, J.M. Synucleins in synaptic plasticity and neurodegenerative disorders. *J. Neurosci. Res.* **1999**, *58*, 120–129. [[CrossRef](#)]
2. Burré, J.; Sharma, M.; Tsetsenis, T.; Buchman, V.; Etherton, M.R.; Südhof, T.C. α -Synuclein promotes SNARE-complex assembly in vivo and in vitro. *Science* **2010**, *329*, 1663–1667. [[CrossRef](#)]
3. Burré, J. The Synaptic Function of α -Synuclein. *J. Park. Dis.* **2015**, *5*, 699–713. [[CrossRef](#)] [[PubMed](#)]
4. Polymeropoulos, M.H. Mutation in the α -Synuclein Gene Identified in Families with Parkinson's Disease. *Science* **1997**, *276*, 2045–2047. [[CrossRef](#)] [[PubMed](#)]
5. Visanji, N.P.; Brotchie, J.M.; Kalia, L.V.; Koprach, J.B.; Tandon, A.; Watts, J.C.; Lang, A.E. α -Synuclein-Based Animal Models of Parkinson's Disease: Challenges and Opportunities in a New Era. *Trends Neurosci.* **2016**, *39*, 750–762. [[CrossRef](#)] [[PubMed](#)]
6. Venda, L.L.; Cragg, S.J.; Buchman, V.L.; Wade-Martins, R. α -Synuclein and dopamine at the crossroads of Parkinson's disease. *Trends Neurosci.* **2010**, *33*, 559–568. [[CrossRef](#)] [[PubMed](#)]

7. Chandra, S.; Fornai, F.; Kwon, H.-B.; Yazdani, U.; Atasoy, D.; Liu, X.; Hammer, R.E.; Battaglia, G.; German, D.C.; Castillo, P.E.; et al. Double-knockout mice for alpha- and beta-synucleins: Effect on synaptic functions. *Proc. Natl. Acad. Sci. USA* **2004**, *101*, 14966–14971. [[CrossRef](#)] [[PubMed](#)]
8. Robertson, D.C.; Schmidt, O.; Ninkina, N.; Jones, P.A.; Sharkey, J.; Buchman, V.L. Developmental loss and resistance to MPTP toxicity of dopaminergic neurones in substantia nigra pars compacta of γ -synuclein, α -synuclein and double α/γ -synuclein null mutant mice. *J. Neurochem.* **2004**, *89*, 1126–1136. [[CrossRef](#)] [[PubMed](#)]
9. Maroteaux, L.; Campanelli, J.T.; Scheller, R.H. Synuclein: A neuron-specific protein localized to the nucleus and presynaptic nerve terminal. *J. Neurosci.* **1988**, *8*, 2804–2815. [[CrossRef](#)]
10. Al-Wandi, A.; Ninkina, N.; Millership, S.J.; Williamson, S.J.; Jones, P.A.; Buchman, V.L. Absence of α -synuclein affects dopamine metabolism and synaptic markers in the striatum of aging mice. *Neurobiol. Aging* **2010**, *31*, 796–804. [[CrossRef](#)]
11. Connor-Robson, N.; Peters, O.; Millership, S.; Ninkina, N.; Buchman, V.L. Combinational losses of synucleins reveal their differential requirements for compensating age-dependent alterations in motor behavior and dopamine metabolism. *Neurobiol. Aging* **2016**, *46*, 107–112. [[CrossRef](#)] [[PubMed](#)]
12. Ninkina, N.; Tarasova, T.V.; Chapro, K.D.; Roman, A.Y.; Kukharsky, M.S.; Kolik, L.G.; Ovchinnikov, R.; Ustyugov, A.A.; Durnev, A.D.; Buchman, V.L. Alterations in the nigrostriatal system following conditional inactivation of α -synuclein in neurons of adult and aging mice. *Neurobiol. Aging* **2020**, *91*, 76–87. [[CrossRef](#)] [[PubMed](#)]
13. Greten-Harrison, B.; Polydoro, M.; Morimoto-Tomita, M.; Diao, L.; Williams, A.M.; Nie, E.H.; Makani, S.; Tian, N.; Castillo, P.E.; Buchman, V.L.; et al. $\alpha\beta\gamma$ -Synuclein triple knockout mice reveal age-dependent neuronal dysfunction. *Proc. Natl. Acad. Sci. USA* **2010**, *107*, 19573–19578. [[CrossRef](#)]
14. Anwar, S.; Peters, O.; Millership, S.J.; Ninkina, N.; Doig, N.; Connor-Robson, N.; Threlfell, S.; Kooner, G.; Deacon, R.M.; Bannerman, D.M.; et al. Functional alterations to the nigrostriatal system in mice lacking all three members of the synuclein family. *J. Neurosci.* **2011**, *31*, 7264–7274. [[CrossRef](#)] [[PubMed](#)]
15. Tomić, S.; Rajkovic, I.; Pekic, V.; Salha, T.; Misevic, S. Impact of autonomic dysfunctions on the quality of life in Parkinson’s disease patients. *Acta Neurol. Belg.* **2016**, *117*, 207–211. [[CrossRef](#)] [[PubMed](#)]
16. Merola, A.; Romagnolo, A.; Rosso, M.; Suri, R.; Berndt, Z.; Maule, S.; Lopiano, L.; Espay, A.J. Autonomic dysfunction in Parkinson’s disease: A prospective cohort study. *Mov. Disord.* **2018**, *33*, 391–397. [[CrossRef](#)]
17. Micieli, G.; Tosi, P.; Marcheselli, S.; Cavallini, A. Autonomic dysfunction in Parkinson’s disease. *Neurol. Sci.* **2003**, *24*, s32–s34. [[CrossRef](#)]
18. Braak, H.; Del Tredici, K.; Rüb, U.; De Vos, R.A.; Steur, E.N.J.; Braak, E. Staging of brain pathology related to sporadic Parkinson’s disease. *Neurobiol. Aging* **2003**, *24*, 197–211. [[CrossRef](#)]
19. Braak, H.; Sastre, M.; Bohl, J.R.E.; De Vos, R.A.I.; Del Tredici, K. Parkinson’s disease: Lesions in dorsal horn layer I, involvement of parasympathetic and sympathetic pre- and postganglionic neurons. *Acta Neuropathol.* **2007**, *113*, 421–429. [[CrossRef](#)]
20. Kaufmann, H.; Nahm, K.; Purohit, D.; Wolfe, D. Autonomic failure as the initial presentation of Parkinson disease and dementia with Lewy bodies. *Neurology* **2004**, *63*, 1093–1095. [[CrossRef](#)]
21. Metzger, J.M.; Emborg, M. Autonomic dysfunction in Parkinson disease and animal models. *Clin. Auton. Res.* **2019**, *29*, 397–414. [[CrossRef](#)] [[PubMed](#)]
22. Onodera, M.; Kuwaki, T.; Kumada, M.; Masuda, Y. Determination of Ventilatory Volume in Mice by Whole Body Plethysmography. *Jpn. J. Physiol.* **1997**, *47*, 317–326. [[CrossRef](#)] [[PubMed](#)]
23. Sheikhabaehi, S.; Gourine, A.V.; Smith, J.C. Respiratory rhythm irregularity after carotid body denervation in rats. *Respir. Physiol. Neurobiol.* **2017**, *246*, 92–97. [[CrossRef](#)] [[PubMed](#)]
24. Sheikhabaehi, S.; Turovsky, E.A.; Hosford, P.S.; Hadjihambi, A.; Theparambil, S.M.; Liu, B.; Marina, N.; Teschemacher, A.G.; Kasparov, S.; Smith, J.C.; et al. Astrocytes modulate brainstem respiratory rhythm-generating circuits and determine exercise capacity. *Nat. Commun.* **2018**, *9*, 370. [[CrossRef](#)] [[PubMed](#)]
25. Feng, M.; Whitesall, S.; Zhang, Y.; Beibel, M.; Alecy, L.D.; DiPetrillo, K. Validation of Volume-Pressure Recording Tail-Cuff Blood Pressure Measurements. *Am. J. Hypertens.* **2008**, *21*, 1288–1291. [[CrossRef](#)] [[PubMed](#)]
26. David, J.M.; Chatziioannou, A.F.; Taschereau, R.; Wang, H.; Stout, D.B. The Hidden Cost of Housing Practices: Using Noninvasive Imaging to Quantify the Metabolic Demands of Chronic Cold Stress of Laboratory Mice. *Comp. Med.* **2013**, *63*, 386–391.

27. Devine, M.J.; Gwinn-Hardy, K.; Singleton, A.; Hardy, J. Parkinson's disease and α -synuclein expression. *Mov. Disord.* **2011**, *26*, 2160–2168. [[CrossRef](#)]
28. Martin, I.; Dawson, V.L.; Dawson, V.L. Recent advances in the genetics of Parkinson's disease. *Annu. Rev. Genom. Hum. Genet.* **2011**, *12*, 301–325. [[CrossRef](#)]
29. Eschbach, J.; Danzer, K.M. α -Synuclein in Parkinson's disease: Pathogenic function and translation into animal models. *Neurodegener. Dis.* **2014**, *14*, 1–17. [[CrossRef](#)]
30. Lee, Y.; Dawson, V.L.; Dawson, T.M. Animal Models of Parkinson's Disease: Vertebrate Genetics. *Cold Spring Harb. Perspect. Med.* **2012**, *2*, a009324. [[CrossRef](#)]
31. Crabtree, D.M.; Zhang, J. Genetically engineered mouse models of Parkinson's disease. *Brain Res. Bull.* **2012**, *88*, 13–32. [[CrossRef](#)] [[PubMed](#)]
32. Chesselet, M.-F.; Richter, F. Modelling of Parkinson's disease in mice. *Lancet Neurol.* **2011**, *10*, 1108–1118. [[CrossRef](#)]
33. Duty, S.; Jenner, P. Animal models of Parkinson's disease: A source of novel treatments and clues to the cause of the disease. *Br. J. Pharmacol.* **2011**, *164*, 1357–1391. [[CrossRef](#)] [[PubMed](#)]
34. Chinta, S.J.; Mallajosyula, J.K.; Rane, A.; Andersen, J.K. Mitochondrial alpha-synuclein accumulation impairs complex I function in dopaminergic neurons and results in increased mitophagy in vivo. *Neurosci. Lett.* **2010**, *486*, 235–239. [[CrossRef](#)]
35. Mullin, S.; Schapira, A.H.V. α -Synuclein and mitochondrial dysfunction in Parkinson's disease. *Mol. Neurobiol.* **2013**, *47*, 587–597. [[CrossRef](#)]
36. Chaturvedi, R.K.; Beal, M.F. Mitochondrial Diseases of the Brain. *Free Radic. Boil. Med.* **2013**, *63*, 1–29. [[CrossRef](#)]
37. Di Maio, R.; Barrett, P.J.; Hoffman, E.K.; Barrett, C.W.; Zharikov, A.; Borah, A.; Hu, X.; McCoy, J.; Chu, C.T.; Burton, E.A.; et al. α -Synuclein binds to TOM20 and inhibits mitochondrial protein import in Parkinson's disease. *Sci. Transl. Med.* **2016**, *8*, 342ra78. [[CrossRef](#)]
38. Angelova, P.R.; Kasymov, V.; Christie, I.; Sheikhabaei, S.; Turovsky, E.; Marina, N.; Korsak, A.; Zwicker, J.; Teschemacher, A.G.; Ackland, G.L.; et al. Functional Oxygen Sensitivity of Astrocytes. *J. Neurosci.* **2015**, *35*, 10460–10473. [[CrossRef](#)]
39. Gourine, A.V.; Funk, G.D. On the existence of a central respiratory oxygen sensor. *J. Appl. Physiol.* **2017**, *123*, 1344–1349. [[CrossRef](#)]
40. Smith, J.C.; Ellenberger, H.H.; Ballanyi, K.; Richter, D.W.; Feldman, J.L. Pre-Bötzinger complex: A brainstem region that may generate respiratory rhythm in mammals. *Science* **1991**, *254*, 726–729. [[CrossRef](#)]
41. Del Negro, C.A.; Funk, G.D.; Feldman, J.L. Breathing matters. *Nat. Rev. Neurosci.* **2018**, *19*, 351–367. [[CrossRef](#)] [[PubMed](#)]
42. Rajani, V.; Zhang, Y.; Jalubula, V.; Rancic, V.; Sheikhabaei, S.; Zwicker, J.D.; Pagliardini, S.; Dickson, C.; Ballanyi, K.; Kasparov, S.; et al. Release of ATP by pre-Bötzinger complex astrocytes contributes to the hypoxic ventilatory response via a Ca²⁺-dependent P2Y₁ receptor mechanism. *J. Physiol.* **2017**, *596*, 3245–3269. [[CrossRef](#)] [[PubMed](#)]
43. Ludtmann, M.H.R.; Angelova, P.R.; Ninkina, N.; Gandhi, S.; Buchman, V.L.; Abramov, A.Y. Monomeric Alpha-Synuclein Exerts a Physiological Role on Brain ATP Synthase. *J. Neurosci.* **2016**, *36*, 10510–10521. [[CrossRef](#)] [[PubMed](#)]
44. Nakamura, K. α -Synuclein and Mitochondria: Partners in Crime? *Neurotherapeutics* **2013**, *10*, 391–399. [[CrossRef](#)]
45. Tuppy, M.; Barna, B.; Alves-Dos-Santos, L.; Britto, L.; Chiavegatto, S.; Moreira, T.; Takakura, A.C. Respiratory deficits in a rat model of Parkinson's disease. *Neuroscience* **2015**, *297*, 194–204. [[CrossRef](#)]
46. Andrzejewski, K.; Budzińska, K.; Kaczyńska, K. Phrenic and hypoglossal nerve activity during respiratory response to hypoxia in 6-OHDA unilateral model of Parkinson's disease. *Life Sci.* **2017**, *180*, 143–150. [[CrossRef](#)]
47. Oliveira, L.M.; Tuppy, M.; Moreira, T.S.; Takakura, A.C. Role of the locus coeruleus catecholaminergic neurons in the chemosensory control of breathing in a Parkinson's disease model. *Exp. Neurol.* **2017**, *293*, 172–180. [[CrossRef](#)]
48. Lima, J.C.; Oliveira, L.M.; Botelho, M.T.; Moreira, T.S.; Takakura, A.C. The involvement of the pathway connecting the substantia nigra, the periaqueductal gray matter and the retrotrapezoid nucleus in breathing control in a rat model of Parkinson's disease. *Exp. Neurol.* **2018**, *302*, 46–56. [[CrossRef](#)]

49. Oliveira, L.M.; Oliveira, M.A.; Moriya, H.T.; Moreira, T.S.; Takakura, A.C. Respiratory disturbances in a mouse model of Parkinson's disease. *Exp. Physiol.* **2019**, *104*, 729–739. [[CrossRef](#)]
50. Machhada, A.; Ang, R.; Ackland, G.L.; Ninkina, N.; Buchman, V.L.; Lythgoe, M.F.; Trapp, S.; Tinker, A.; Marina, N.; Gourine, A.V. Control of ventricular excitability by neurons of the dorsal motor nucleus of the vagus nerve. *Hear. Rhythm.* **2015**, *12*, 2285–2293. [[CrossRef](#)]
51. Wirth, A.; Wang, S.; Takefuji, M.; Tang, C.; Althoff, T.F.; Schweda, F.; Wettschureck, N.; Offermanns, S. Age-dependent blood pressure elevation is due to increased vascular smooth muscle tone mediated by G-protein signaling. *Cardiovasc. Res.* **2015**, *109*, 131–140. [[CrossRef](#)] [[PubMed](#)]
52. Moreira, T.S.; Antunes, V.R.; Falquetto, B.; Marina, N. Long-term stimulation of cardiac vagal preganglionic neurons reduces blood pressure in the spontaneously hypertensive rat. *J. Hypertens.* **2018**, *36*, 2444–2452. [[CrossRef](#)] [[PubMed](#)]
53. Hotta, H.; Uchida, S. Aging of the autonomic nervous system and possible improvements in autonomic activity using somatic afferent stimulation. *Geriatr. Gerontol. Int.* **2010**, *10*, S127–S136. [[CrossRef](#)] [[PubMed](#)]
54. Mancia, G.; Grassi, G. The Autonomic Nervous System and Hypertension. *Circ. Res.* **2014**, *114*, 1804–1814. [[CrossRef](#)] [[PubMed](#)]
55. Palma, J.-A.; Kaufmann, H. Treatment of autonomic dysfunction in Parkinson disease and other synucleinopathies. *Mov. Disord.* **2018**, *33*, 372–390. [[CrossRef](#)]
56. Isonaka, R.; Rosenberg, A.Z.; Sullivan, P.; Corrales, A.; Holmes, C.; Sharabi, Y.; Goldstein, D.S. Alpha-Synuclein Deposition Within Sympathetic Noradrenergic Neurons Is Associated With Myocardial Noradrenergic Deficiency in Neurogenic Orthostatic Hypotension. *Hypertension* **2019**, *73*, 910–918. [[CrossRef](#)]



© 2020 by the authors. Licensee MDPI, Basel, Switzerland. This article is an open access article distributed under the terms and conditions of the Creative Commons Attribution (CC BY) license (<http://creativecommons.org/licenses/by/4.0/>).